Journal of Applied Polymer Science

A Novel Lead Ion-Imprinted Chelating Nanofiber: Preparation, Characterization, and Performance Evaluation

Lanyan Tong,[1] Jida Chen,[1] Youyou Yuan,[1] Zehua Cui,[1] Mianfu Ran,[1] Qian Zhang,[1] Juan Bu,[2] Fengqing Yang,[1] Xinhong Su,[3] Huan Xu[4]

[1]School of Chemistry and Chemical Engineering, Chongqing University, Chongqing, People's Republic of China
[2]Chongqing Police College, Chongqing, People's Republic of China
[3]Zhuhai Founder Technology Multilayer PCB. Co., Ltd, Guangdong, People's Republic of China
[4]Bomin Electronics Co., Ltd, Guangdong, People's Republic of China
Correspondence to: J. Chen (E-mail: chencqu@cqu.edu.cn)

ABSTRACT: A novel Pb(II) ion-imprinted chelating nanofibers (nIIP), synthesized by combining electrospinning with surface ion imprinting technique, was reported in this study. nIIP was characterized with Fourier transmission infrared spectrometry and scanning electron microscopy, respectively. The performance of nIIP for Pb(II) sorption was conducted through a batch adsorption experiments. Experimental data showed that adsorption capacity of nIIP was much higher than that of non-ion imprinted chelating acrylic microfibers (mNIP) derived from commercial available acrylic microfibers, and adsorption behaviors agreed well with pseudo-second-order kinetic and Langmuir isotherm model. The values of Gibbs free energy change derived from experimental data suggested that the adsorption Pb(II) on nIIP is spontaneous and favorable at high temperature. In addition, nIIP had the highest selectivity among three tested fibrous adsorbents for Pb(II) from binary metal solution, the selectivity coefficients for Pb(II) from binary metal solution of Pb(II)/Cu(II), Pb(II)/Ni(II), and Pb(II)/Cd(II) onto nIIP were 47, 101, and 162, respectively. Besides, a forty adsorption/desorption cycles revealed that nIIP was a promising recyclable adsorbent. In conclusion, the novel nIIP is a highly effective adsorbent for enrichment and separation of Pb(II) in the presence of competitive ions in aqueous solution, and it is potential to be applied for recovering metals from heavy metal polluted industrial wastewater such as Pb(II)/Cd(II), Pb(II)/Ni(II), and Pb(II)/Cu(II) polluted wastewater. © 2014 Wiley Periodicals, Inc. J. Appl. Polym. Sci. **2015**, *132*, 41507.

KEYWORDS: adsorption; fibers; separation techniques

Received 29 May 2014; accepted 7 September 2014
DOI: 10.1002/app.41507

INTRODUCTION

Heavy metal pollution of water has been increasing with industrial growth and development in recent years,[1] which aroused serious public health concerns[2–7] because heavy metal ions cannot be degraded and tend to enter food chains through accumulation in organisms. On the other hand, heavy metal pollution of water is actually natural resource of metals as waste forms discharged into water. Therefore, an ideal strategy for treatment of metal polluted wastewater should be recycle or recover metals while environmental protect action is performed. Unfortunately, this kind of techniques has not occured at present due to technical difficulties.[8–10] For instance, chemical precipitation is one of the most commom used techniques for wastewater treatment, which is based only on changing soluble metal ions into insolubles as sludge, and the metals in sludge have never been considered to be recycled or recovered mainly due to technical and economic problems. What's more, this kind of sludge required to be further treated resulting in extra cost and low efficiency. Adsorption method has been recongnized as a potential technique for recycling or recovering metal resources from wastewater,[11] however, the recovered metals are useless partially owing to impurity while a traditionally nonselctivive adsorbents are applied. To improve the capability of selective extraction and accumulation of metals with adsorption technique, many researchers have devoted to develop selective adsorbents and made some progress by ion imprinting on small scale substrates such as nanoparticles or microspheres.[12–14]

Ion imprinting, which is derived from molecular imprinting technique[15] and has been extensively applied in scientific fields,[16–18] is a feasible and powerful technique for creating tailor-made binding sites for target ions. For instance, Wang and coworkers[19–24] prepared recycable and applied for separation and enrichment of Pb(II) in wastewater, the maximum adsorption capacity of Pb(II) was up to 221 mg/g. However, there are two main issues that must be considered for selective adsorbents in the form of small particles, that is, rapidly rising

fluid resistance and difficulty in particle separation and recycling. Compared to small scale granular adsorbents, fibrous adsorbents, nanofibers can be easily separated and recycled, which possess characteristics such as large external surface area, short transit distance, low pressure drops, and flexibility in adsorption process. In addition, a fibrous adsorbent can be prepared in various forms (including fibers, films, filters, and nonwoven fabric, etc). Most importantly, nanofibers are ready to be produced by electrospinning technique.[25–27] Therefore, it is of great interest to develop selectively fibrous adsorbents for wastewater treatment and recovering pure metals.

In the current study, a newly surface Pb(II) ion-imprinted chelating nanofiber (nIIP) was prepared for selective adsorption and accumulation of Pb(II) from aqueous solution. Typically, electrospun polyacrylonitrile (PAN) nanofibers as substrate was crosslinked with diethylenetriamine (DETA), functionalized with hydroxylamine hydrochloride, and imprinted with Pb(II) as a template subsequently. The harvested nIIP was characterized with Fourier transform infrared spectroscopy (FTIR) and scanning electron microscopy (SEM), respectively. The adsorption performance of nIIP was systemically investigated.

EXPERIMENTAL

Materials

PAN (repeat unit is —CH_2CHCN—, unit weight 53, acrylonitrile $\geq$ 99%, molecular weight 90,000) was supplied by Kunshan Hongyu Plastics Co., Ltd (China). For comparative purposes, a commercial available fiber with diameter of 25–133 μm called acrylic fibers, a copolymer of 85 mol % acrylonitrile monomer, and 15 mol % methylacrylate monomer was purchased from Binzhou Qidong Carbon Materials Co. (China), which was washed with methanol and distilled water successively before use. Other chemicals such as glutaraldehyde, hydrochloric acid, dimethylformamide (DMF), hydroxylamine hydrochloride ($NH_2OH{\cdot}HCl$), DETA, ethanediol, sodium hydroxide, lead nitrate ($Pb(NO_3)_2$), copper nitrate ($Cu(NO_3)_2$), nickel nitrate ($Ni(NO_3)_2$), and cadmium nitrate ($Cd(NO_3)_2$) were of analytical grade and used without further purification.

Preparation of Fibrous Adsorbents

Electrospinning of PAN Nanofibers. PAN nanofibers were prepared according to method reported by Saeeda et al.[28] with minor modifications. Briefly, a homogeneous PAN solution of 10 wt % was prepared by dissolving as-received PAN in DMF at 90°C under stirring for 5–6 h, and kept stirring at room temperature for another 12 h before loaded to a 5-mL glass syringe with a needle tip 0.55 (tip inner diameter was 0.55 mm) for electrospinning. The feeding rate of the PAN solution was 0.5 mL/h, which was controlled by a syringe pump. A voltage of 23 kV was applied to the needle, and the distance between needle tip and collector was 8 cm. Jets of the PAN solution came out from the needle tip, which were collected onto an aluminum (Al) sheet wrapped around a rotating cylinder at room temperature. When the solvent evaporated, non-woven electrospun PAN nanofibers were formed.

Crosslinking and Amidoximation Fibrous PAN. Fibrous PAN was crosslinked before amidoximation, and the crosslinking reaction was based on amination of PAN as shown in Scheme 1(a).[29] Briefly, about 0.2 g of fibrous PAN (electrospun PAN nanofibers, or commercial acrylic mictrofibers) was placed into a sealed chamber containing 0.36 mL of DETA and 46 mL of ethanediol. Crosslinking reaction was carried out at 80°C for 3 h. After the reaction, crosslinked fibrous PAN was washed with distilled water, and then air-dried overnight before applied for amidoximation.

The amidoximation reaction[30,31] was based on reaction of nitrile groups on fibrous PAN with hydroxylamine hydrochloride as illustrated in Scheme 1(b). Briefly, about 0.2 g crosslinked fibrous PAN (crosslinked electrospun PAN nanofibers, or crosslinked acrylic mictrofibers) was put into a flask equipped with a reflux condenser and containing 30 mL hydroxylamine hydrochloride aqueous solution of 3 g/L, the pH value of solution was controlled at 6.8 with saturated sodium carbonate solution, and the amidoximation reaction was carried out under stirring at 70°C for 3 h. The amidoximated electrospun PAN nanofibers (hereafter, called as non-ion imprinted PAN chelating nanofibers or nNIP) and amidoximated acrylic fibers (hereafter, called as non-ion imprinted PAN chelating acrylic mictrofibers or mNIP) were separated by filtration, washed with distilled water till no participate were formed through silver ion experiment to check no residual chloride ion in effluent solution, and dried in a vacuum oven at 40°C before use.

Pb(II) Imprinting Fibrous PAN. To prepare Pb(II) ion-imprinted fibrous adsorbent (hereafter, called as nIIP), about 0.1 g nNIP was immersed in 100 mL of 500 mg/L Pb(II) aqueous solution at pH 5.8 (by acetate buffer solution) for 2 h, seperated and washed with distilled water to remove redundant Pb(II) on fibers, crosslinked with 2 wt % glutaraldehyde aqueous solution at room temperature for 2 h.[32,33] At the end of reactions, the resulting nanofibers were collected and washed with 0.1 mol/L HCl to remove the template ion of Pb(II), washed further with distilled water and dried in a vacuum oven at 40°C for 24 h to harvest nIIP. Actually surface ion imprintrd technique was studied by Gao et al.[19] including binding curves of surface ion imprinted polymer toward template ions and using HCl solution as eluent. The supposed Pb(II) ion imprinting reactions[31] are illustrated in Scheme 1(c).

Characterization

Functional groups of fibrous adsorbents were identified with Fourier transform infrared spectrometry (IR Affinity^{-1}, SHIMADZU, Japan) based on KBr method, with a resolution of 4 cm^{-1} and a wavenumber range of 4000–400 cm^{-1}. Morphology of samples, namely electrospun PAN nanofibers, nNIP, and nIIP, were observed and recorded with SEM (JSM-5600LV, Japan).

Adsorption Experiments

Adsorption of Pb(II). All adsorption experimentals of fibrous adsorbents were carried out as follow. Briefly, fibrous adsorbents were weighted (W), mmersed into Pb(II) solutions (volume V, initial concentration C_0), and the solution was stirred continuously with a magnetic stirrer for 3 h for complete adsorption equilibration (equilibrium concentration C_e), residual Pb(II) in solution was determined by atomic absorption spectroscopy (180-80 HITACHI, Japan). The effect of solution pH on Pb(II) sorption was carried out in Pb(II) solution of 500 mg/L at the pH

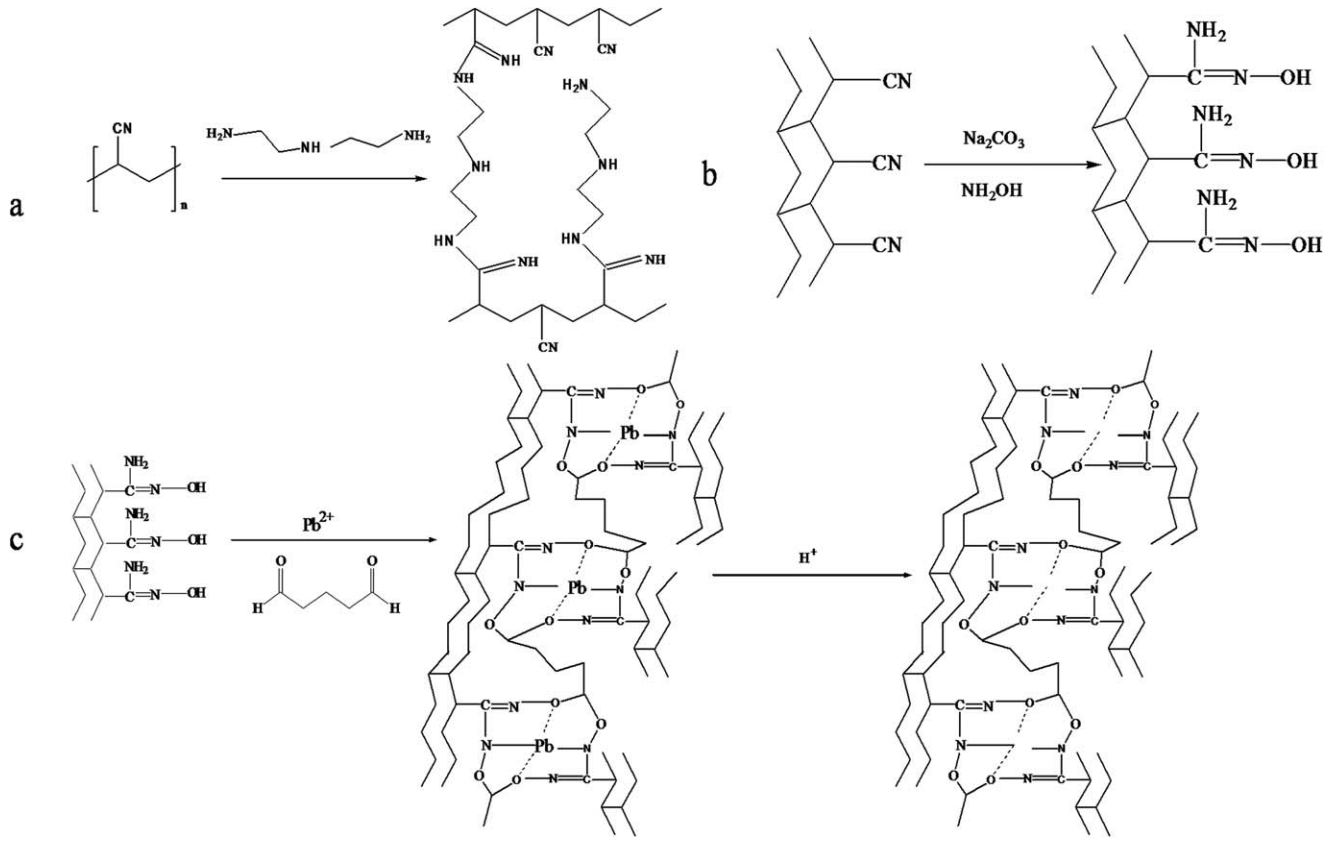

Scheme 1. (a)The crosslinking reaction of PAN fibers; (b)The amidoximation reaction of PAN fibers. (c) The supposed Pb(II) imprinting reactions.

range of 2.6–6.6. The initial pH of solution was adjusted with acetate buffer solutions. For determining the effect of contact time on Pb(II) sorption, the experiments were done in Pb(II) solution of 200 mg/L and pH 5.8 at definite intervals. For examining the effect of initial Pb(II) concentration and temperature, the experiments were carried out in Pb(II) solution of initial concentration range from 100 to 800 mg/L and pH 5.8 at four different temperatures (15, 25, 35, and 45°C). Each experiment was repeated three times and the results were given as averages.

The absorption capacity q_e (mg/g) at equilibrium, and adsorption amount q_t (mg/g) at time t (min) were calculated on the basis of the following equations:

$$q_e = \frac{(C_0 - C_e)V}{W} \quad (1)$$

$$q_t = \frac{(C_0 - C_t)V}{W} \quad (2)$$

where C_0 (mg/L), C_e (mg/L), and C_t (mg/L) are the Pb(II) concentrations at initial, time t, and equilibrium, respectively. V (L) and W (g) are the volume of solution and the weight of fibrous adsorbent, respectively.

Selective Adsorption. Competitive sorption of fibrous adsorbents was investigated in binary metal ion solutions. Briefly, fibrous adsorbents were weighted (W), immersed into solutions (volume V) of binary metal ions (Pb(II)/Cu(II), Pb(II)/Ni(II), and Pb(II)/Cd(II)) containing equal amount (2.415 mmol/L) of each metal at pH 5.8, and the solution was stirred continuously with a magnetic stirrer for 3 h for complete adsorption equilibration (equilibrium concentration C_e). Concentrations of ions in solutions were determined by atomic absorption spectroscopy (180-80 HITACHI, Japan). Distribution coefficient K_d (L/g) and selective coefficient k were calculated on the basis of following equations[34]:

$$K_d = \frac{(C_0 - C_e) \times V}{C_e \times W} \quad (3)$$

$$k' = \frac{K_{d(\mathrm{Pb})}}{K_{d(\mathrm{M})}} \quad (4)$$

where C_0 (mg/L) and C_e(mg/L) are the concentration of metal ions at initial and equilibrium in solution, respectively. V (L) is the volume of binary metal ion solution, and W (g) denotes the weight of adsorbent. $K_{d(\mathrm{Pb})}$ (L/mg) and $K_{d(\mathrm{M})}$ (L/mg) are the distribution of Pb(II) and M(II), respectively. k' denotes the selectivity coefficient of Pb(II) over M(II).

Adsorption/Desorption Experiments

Adsorption/desorption of Pb(II) on fibrous adsorbents was conducted according to previous report with some modifications.[28] Briefly, Pb(II) loaded fibrous adsorbents were placed in a 50 mL hydrochloride solution with concentration of 0.1 mol/L at 25°C under stirring for 2 h, then the fibers were filtrated out, washed with distilled water till no cholride ions in effluent solution detected through silver ion experiment, subjected again to

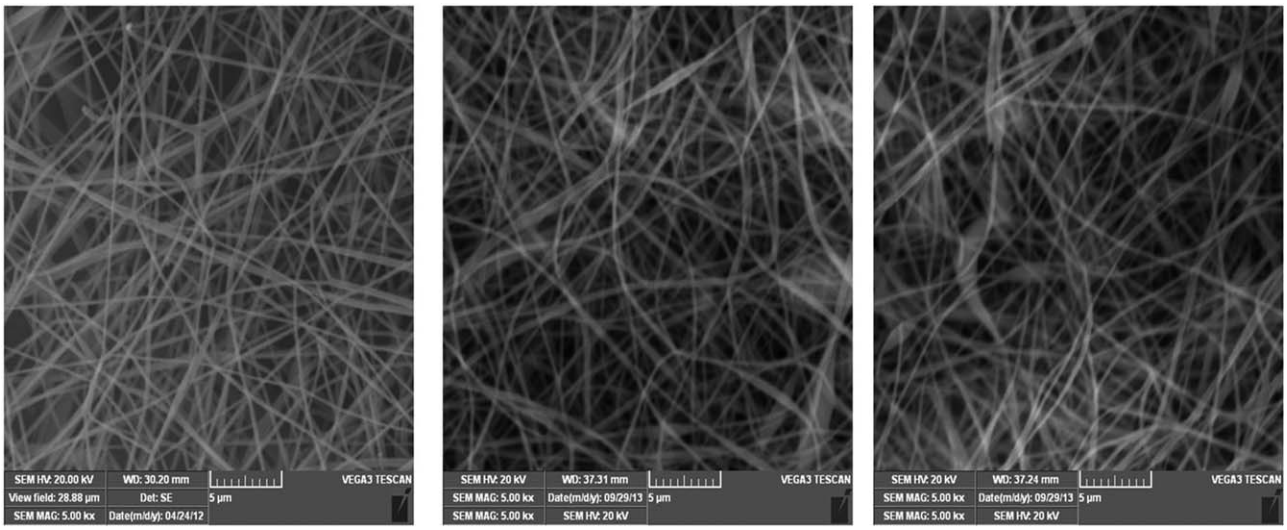

Figure 1. SEM images of nanofibers: (a) electrospun PAN nanofibers; (b) nNIP nanofibers; (c) nIIP.

adsorption process in Pb(II) solution of 500 mg/L at pH 5.8 for forty cycles. Residual Pb(II) in solution was determined by atomic absorption spectroscopy. The relative adsorption capacity (R) was calculated on the basis of the following equation.

$$R = \frac{q_{e(n)}}{q_{e(1)}} \times 100\% \quad (5)$$

where $q_{e(1)}$ and $q_{e(n)}$ denote the absorption capacity (mg/g) of adsorption/desorption cycle one and cycle n, respectively.

RESULTS AND DISCUSSION

Characterization of Samples

Morphologies of electrospun PAN nanofibers, nNIP, and nIIP were observed by SEM, and the images are shown in Figure 1. Evidently, Figure 1(a) showed that electrospun PAN nanofibers were round at cross-sections and with smooth surfaces. The diameter of the nanofibers was rather uniform with the values from 300 to 400 nm, which was comparable to that reported by Saeed et al.[28]. Figure 1(b) shows the morphology of nNIP. It was shown that the diameter of NIP nanofibers increased and became uneven compared with those of electrospun PAN nanofibers owing to chemical reactions of crosslinking and amidoximation, and the morphological changes were similar to that reported by Saeed et al.[28]. Compared to nNIP, morphologies of nIIP, as shown in Figure 1(c), were not significantly changed although there was a chemical reaction taking place at room temperature for 2 h. The experimental results suggested that the major factors that caused morphological changes of nanofibers should be reaction temperature and time.

The FTIR spectra of samples are shown in Figure 2. Figure 2(A) is the spectra of nNIP, spectrum of electrospun PAN nanofibers (spectrum a) exhibited strong adsorption peaks at 2242 cm^{-1}, corresponding to stretching vibrations of nitrile groups of PAN.[35] The spectrum of crosslinked PAN nanofibers (spectrum b) illustrated that the strength of bands at ~3400 and ~1600 cm^{-1} was increased, which can be assigned to stretching vibrations of amine group (N—H) and the amidine group (C=N) resulting from crosslinked reaction between nitrile and DETA. At the same time, the intensity of peak at 2242 cm^{-1} decreased, which implied that there were only part of nitrile groups crosslinked with DETA. After amidoximation reaction of crosslinked PAN nanofibers with hydroxylamine, a sharp band presented at 915 cm^{-1} in the spectrum of nNIP (spectrum c), which can be attributed to bending vibration of N—O.[28] In general, the FTIR spectra in Figure 2(A) confirmed that crosslinking and amidoximation of PAN nanofibers were successful.

Figure 2(B) is the spectra of nIIP. The spectrum of nNIP chelating with Pb(II) (spectrum a) exhibited a new adsorption peaks at 1390 cm^{-1} and 1080 cm^{-1} compared with Figure 2(A) (spectrum c) due to –N and –O of amidoxime groups coordination with Pb(II), approving complex of Pb—N and Pb—O.[23] After crosslinking reaction with glutaraldehyde, Figure 2(B) (spectrum b) shows a wider adsorption band at 1010–1200 cm^{-1} corresponding to stretching vibrations of C—O by the introduction of glutaraldehyde. The spectrum of desorption nanofibers (spectrum c), exhibiting the intensity of Pb—N and Pb—O (1390 cm^{-1} and 1080 cm^{-1}), decreased as the deprotonation of Pb—N and Pb—O bond by desorption of HCl. Based on the above analysis, it was concluded that Pb—N and Pb—O groups anticipated to occur in the fabrication of nIIP, clearly weaken after deprotonation of Pb—N and Pb—O bond by desorption of HCl. From the above discussion, the mechanism (Scheme 1) proposed for the preparation of nIIP is suitable.

Adsorption of Pb(II)

Effect of pH on Adsorption. The solution pH is known to be one of the most important factors affecting adsorption capacity of adsorbents, because pH influences protonation of functional groups of adsorbents as well as chemical reaction of heavy metal ions (such as hydrolysis, complexation, and redox reaction). Therefore, solution pH is the most important parameter that

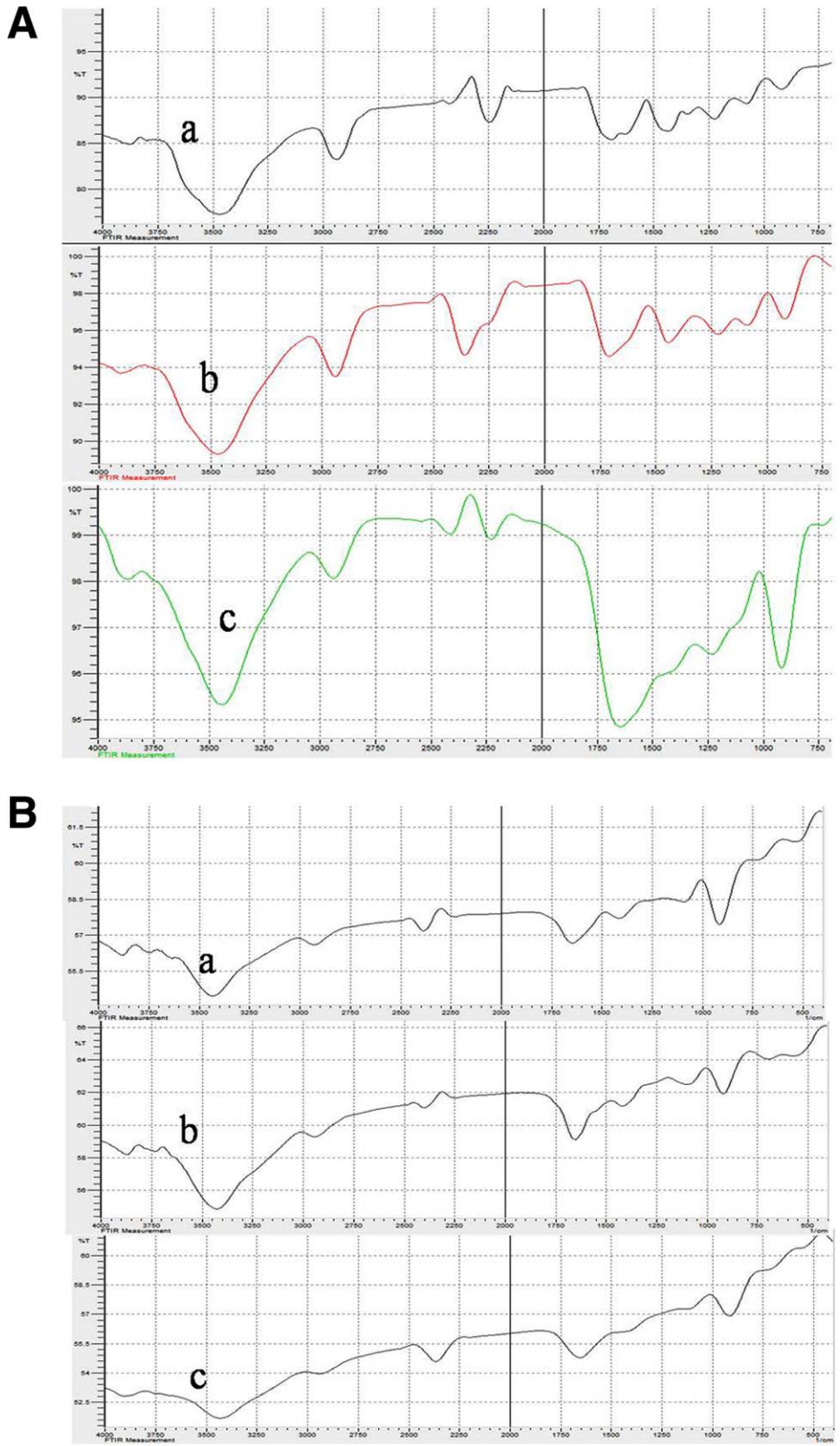

Figure 2. (A) FTIR spectra of fibrous adsorbents: (a) electrospun PAN nanofibers; (b) crosslinked electrospun PAN nanofibers; (c) Nnip. (B) FTIR spectra of Pb(II)-IIP fibrous adsorbents (a) before crosslinking; (b) after crosslinking; (c)after desorption with 0.1 mol/L HCl magnetic stirred at room temperature. [Color figure can be viewed in the online issue, which is available at wileyonlinelibrary.com.]

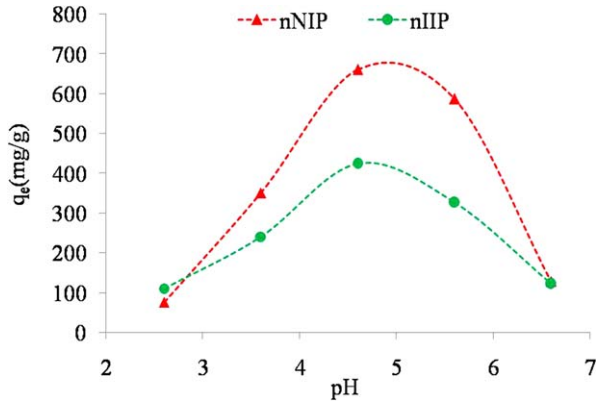

Figure 3. The effect of solution pH on adsorption capacity. [Color figure can be viewed in the online issue, which is available at wileyonlinelibrary.com.]

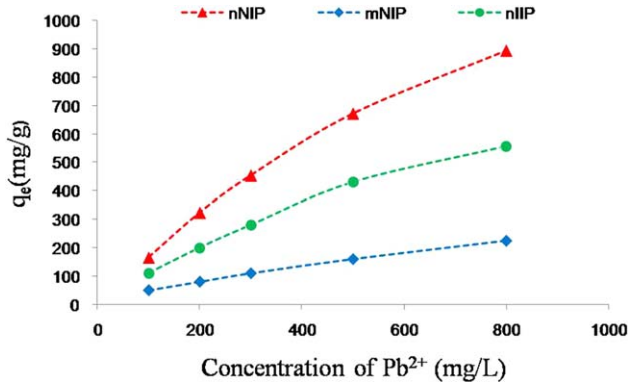

Figure 5. The effect of initial Pb(II) concentration on adsorption capacity. [Color figure can be viewed in the online issue, which is available at wileyonlinelibrary.com.]

should be investigated. It is known that Pb(II) will precipitate in the form of oxides or hydroxides at pH > 7. To avoid precipitation of Pb(II), all adsorption experiments were conducted in Pb(II) solution of 500 mg/L at the pH range of 2.6–6.6.

The effect of solution pH on adsorption capacity of fibrous adsorbents is shown in Figure 3. It is clear that the effect of solution pH on adsorption capacity of nNIP as well as nIIP is significant. At the lowest initial pH investigated, small amounts of Pb(II) could be adsorbed onto adsorbents due particularly to the competitive adsorption between the dominantly available H^+ and Pb(II). As initial pH of the solutions increases, the amounts of Pb(II) adsorbed onto adsorbents increases, and the maximum adsorption capacity (q_e) of both fibers was obtained at pH 4.6 because the functional groups of adsorbents were deprotonated and Pb(II) was attracted to negatively charged groups through electrostatic attraction. To further increase initial pH of solutions, the amounts of Pb(II) adsorbed onto adsorbents decreased, which could be explained that the OH^- ion interacted with Pb(II) to form $Pb(OH)^+$, $Pb_2(OH)_2{}^{2+}$, and $Pb(OH)_2$ resulting in reducing free Pb(II) available.

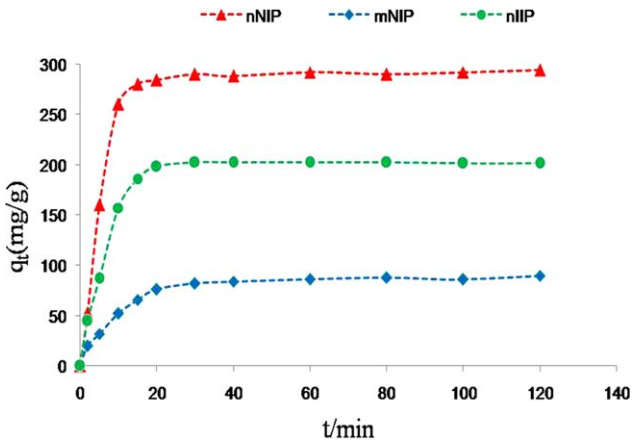

Figure 4. The effect of contact time on adsorption capacity. [Color figure can be viewed in the online issue, which is available at wileyonlinelibrary.com.]

It was also evident that amounts of Pb(II) adsorbed onto nIIP were less than that of nNIP at same experimental conditions as shown in Figure 3, which might be explained that the number of adsorptive sites (functional groups) on nIIP was less than that of nNIP owing to functional group decrease during ion imprinting as shown in Scheme1.

To make sure adsorption efficiency as well as to avoid precipitation of Pb(II), the pH value of solutions was adjusted to 5.8 for subsequent experiments.

Effect of Contact Time on Adsorption. The effect of contact time on adsorption capacity is presented in Figure 4. Generally, there are two steps in adsorption of Pb(II) on fibers. In the initial step, adsorption was swift because of a great number of free adsorptive sites and Pb(II) availability. In the second step, adsorption rates decreased and finally reached to equilibrium owing to depletion of adsorptive sites and Pb(II) in solutions. However, the duration time of initial step of nIIP and nNIP was about 15 min, which was much less than that of mNIP of 40 min. In addition, when the initial Pb(II) concentration was controlled at 200 mg/L, the adsorption capacity of nIIP was 202 mg/g, which was less than that of nNIP (294 mg/g) owing to adsorptive sites decrease resulting from available functional group reduction during ion imprinting process as explained in "Effect of pH on Adsorption." However, adsorption capacity of nIIP was much larger than that of mNIP of 90 mg/g. Those data suggested that fibrous adsorbents in nanoscale (nIIP and nNIP) were much better than fibrous adsorbents in microscale (mNIP) in terms of adsorption rate and capacity.

To ensure the complete adsorption equilibration of Pb(II) on fibrous adsorbents, the contact time of 3 h was chosen for subsequent investigations.

Adsorption Isotherms. The effect of initial Pb(II) concentration on adsorption capacity is shown in Figure 5. It was showed that absorption capacity of nNIP, nIIP, and mNIP increased from 160 to 890 mg/g, 120 to 580 mg/g, and 50 to 225 mg/g, respectively, when initial Pb(II) concentration increased from 100 to 800 mg/L. The results might be explained from two aspects. Firstly, higher initial Pb(II) concentration improves driving force to overcome mass transfer resistance of Pb(II) between

Table I. Isotherm Parameters of Fibrous Adsorbents for Sorption of Pb(II) (pH 5.8; Initial Pb(II) Concentration of 500 mg/L; Temperature of 298 K)

	Model						
	Langmuir				Freundlich		
Fibrous adsorbents	q_m (mg/g)	K (mL/g)	R^2	R_L	K_F	b	R^2
nNIP	1111.1	9.868×10^3	0.996	0.856-0.223	40.36	1.838	0.974
nIIP	1000	2.66×10^3	0.991	0.784-0.429	8.81	1.48	0.989
mNIP	416	1.57×10^3	0.939	0.867-0.44	1.503	1.46	0.999

nNIP, Niip, and mNIP represent non-ion imprinted chelating nanofibers, Pb(II) ion-imprinted chelating nanofibers, and non-ion imprinted chelating microfibers, respectively.

aqueous and solid phases resulting in higher probability of collision between Pb(II) and adsorbents; secondly, the number of adsorptive sites on surface of nIIP and nNIP are much greater than that of mNIP.

Subsequently, two isotherms Langmuir and Freundlich[36,37] were employed to analyze the experimental data. As everyone knows, Langmuir model is based on three assumptions, namely: (1) sorption is limited to monolayer coverage; (2) all surface sites areas are alike, and only can accommodate one adsorbate; (3) the ability of a molecule to be adsorbed on a given site is independent of its neighboring sites occupancy. Langmuir equation is given as follows[23,38]:

$$\frac{C_e}{q_e} = \frac{1}{q_m k_L} + \frac{C_e}{q_m} \tag{6}$$

$$R_L = \frac{1}{1 + C_0 k_L} \tag{7}$$

where q_e (mg/g) is the adsorption amount at equilibrium, C_e (mg/L) is the equilibrium concentration of adsorbate in solution. q_m (mg/g) denotes the maximum adsorption capacity, and K_L (L/mg) is the adsorption intensity or Langmuir coefficient related to affinity of the binding sites. The R_L value indicates whether the type of the isotherm is favorable ($0 < R_L < 1$), unfavorable ($R_L > 1$), linear ($R_L = 1$), or irreversible ($R_L = 0$).

Unlike Langmuir model, Freundlich model is an empirical equation based on sorption on a heterogeneous surfaces or surfaces supporting sites of varied affinities. It is assumed that the stronger binding sites are occupied first and the binding strength decreases with increasing degree of site occupation, and adsorption is not restricted to formation of monolayer. Freundlich model is expressed as follows:

$$\log q_e = \log k_F + \frac{1}{b} \log C_e \tag{8}$$

where k_F and $1/b$ are constants related to adsorption capacity and adsorption intensity, respectively. A smaller $1/b$ value indicates a more heterogeneous surface whereas a value closer to or equal to 1 indicates adsorbent has relatively more homogeneous binding sites. C_e (mg/L) is the equilibrium concentration of adsorbate in solution.

The isotherm parameters of fibrous adsorbents were calculated and presented in Table I. According to the obtained results, the adsorption of Pb(II) on nIIP and nNIP was fitted particularly well with Langmuir model, as indicated by the very high values of correlation coefficient ($R^2 > 0.99$). It revealed that adsorptive sites of nIIP and nNIP were structurally homogeneous and Pb(II) covered their surfaces in monolayer. In addition, maximum adsorption capacity of Pb(II) on nNIP was greater than that of nIIP, and mNIP (see Table I), which should be a direct result of the much greater specific surface area of nNIP.[35] Furthermore, the values of R_L for Langmuir model were between 0 and 1, and Freundlich constants ($1/b$) were smaller than 1, suggesting that adsorption process is favorable.

In contrast to nIIP and nNIP, the experimental data of mNIP were fitted particularly well with Freundlich model, as indicated by the very high values of correlation coefficient ($R^2 = 0.999$). The adsorption model of mNIP was different from that of aminated PAN microfibers reported by Kampalanonwat and Supaphol,[35] which might be attributed to the differences in ingredient of raw materials as well as functional groups between mNIP and aminated PAN microfibers.

To verify the binding sites of nIIP and nNIP were identical, the Scatchard was used to analyze the sorption of nIIP and nNIP. Scatchard equation[39] is expressed as follows:

$$q_e/c_e = (Q_{\max} - q_e)/k_D \tag{9}$$

where $Q_{\max}$ (mg/g) is the apparent maximum number of binding sites, k_D is the dissociation equilibrium constant of binding sites, q_e (mg/g) is the adsorption amount at equilibrium, C_e (mg/L) is the equilibrium concentration of adsorbate in solution. The values of K_D and the $Q_{\max}$ can be calculated from the slope and intercept of the linear line plotted in q_e/C_e versus q_e.

It was observed that Scatchard plots were a single straight line. The linear regression equation of nIIP and nNIP for the linear region is $q_e/C_e = 2.65 - 0.003q_e$ ($R^2 = 0.987$) and $q_e/C_e = 11.42 - 0.01q_e$ ($R^2 = 0.979$) (Table II), respectively. It means that the Scatchard plots was a single straight line, which indicated both binding sites of nIIP and nNIP were identical, also implied there is only a kind of function groups on nIIP and nNIP complex with metal ions.

Table II. Parameters of Scatchard Analysis

Fibers	Scatchard	R^2	K_D (mg/L)	$Q_{\max}$ (mg/g)
nIIP	$Y = -0.003X + 2.65$	0.981	333.3	883
nNIP	$Y = -0.01X + 11.42$	0.979	100	1142

nNIP and nIIP represent non-ion imprinted chelating nanofibers and Pb(II) ion-imprinted chelating nanofibers, respectively.

Table III. Kinetic Parameters of Fibrous Adsorbents for Pb(II) Adsorption (pH 5.8; Initial Pb(II) Concentration of 200 mg/L; Temperature of 298 K)

Fibrous adsorbents	Experimental data $q_{e,exp}$ (mg/g)	Pseudo-first-order equation				Pseudo-second-order equation			
		$q_{e,cal}$ (mg/g)	Deviation (%)	$K_1 \times 10^{-2}$ (min^{-1})	R^2	$q_{e,cal}$ (mg/g)	Deviation (%)	$K_2 \times 10^{-3}$ (g/mg min)	R^2
nNIP	294	249.5	17.8	19.5	0.987	298.5	1.5	1.89	0.999
nIIP	202	239	14.25	42.8	0.989	208	2.97	1.78	0.998
mNIP	90	85	5.9	18.8	0.991	94.6	4.86	1.55	0.997

nNIP, nIIP, and mNIP represent non-ion imprinted chelating nanofibers, Pb(II) ion-imprinted chelating nanofibers, and non-ion imprinted chelating microfibers, respectively.

Adsorption Kinetics

To study the mechanism of adsorption process, the effect of reaction time on the adsorption behavior was further analyzed with kinetic models.[40] The pseudo-first-order kinetic model is rendered that the adsorption rate is proportional to the number of unoccupied adsorptive sites. The pseudo-second-order kinetic model is derived based on the notion that adsorption should relate to squared product of the difference between the number of the equilibrium adsorptive sites available on an adsorbent and that of the occupied sites. The intra-particular diffusion model[41] is derived based on the notion that adsorption should be proportional to the squared time. The models can be written as following equations:

$$\ln(q_e - q_t) = \ln q_e - \frac{k_1}{2.303} t \tag{10}$$

$$\frac{t}{q_t} = \frac{1}{k_2 q_e^2} + \frac{t}{q_e} \tag{11}$$

$$q_t = k_i t^{0.5} + C \tag{12}$$

where q_e (mg/g) and q_t (mg/g) denote adsorption amounts per unit mass of adsorbent at equilibrium and time t (min), respectively. k_1 (min^{-1}) and k_2 (g (mg^{-1} min^{-1})) are rate constants of first order and second order model, respectively. The k_i (mg g^{-1} $min^{-1/2}$) denotes the intra-particular diffusion rate constant and the C represents a constant.

Pseudo-first-order model is rendered the rate of occupation of the adsorption sites to be proportional to the number of unoccupied sites; pseudo-second-order kinetic model is assumed the chemical reaction mechanisms,[42] and that the adsorption rate is controlled by chemical adsorption through sharing or exchange of electrons between the adsorbrate and adsorbent.[43] Parameters of two kinetic models are given in Table III, the experimental data were well fitted with pseudo-second-order kinetic model than pseudo-first-order kinetic model. In addition, the theoretical $q_{e,cal}$ values are obtained from experimental $q_{e,exp}$. Therefore, the adsorption of Pb(II) ions onto nIIP process was a chemical process.

In regards to intra-particular diffusion model,[41] the plots of the q_t versus time $t^{1/2}$ are shown in Figure 6. It was showed that the plots were not linear during the contact time of adsorption process, which implied that intra-particle diffusion were not fitted with the study, and the sorption process took place on the surface of nIIP. The kinetic experiment result proves that this surface ion imprinting technique on chelating nanofibers surfaces possesses obvious advantage of surface ion imprinting and nanofibers.

Adsorption Thermodynamics

The effect of temperature on adsorption capacity of adsorbents is presented in Figure 7. According to the data, adsorption capacity of all tested adsorbents increased gradually with the increase of temperature without exception, which could be explained from two aspects: firstly, as temperature rises, the

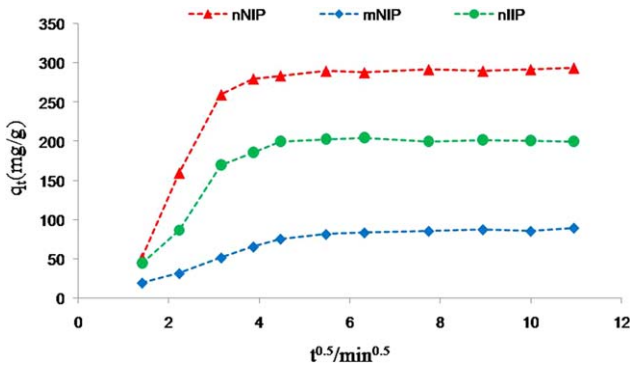

Figure 6. Intra-particular diffusion model of nIIP, nNIP, and mNIP. [Color figure can be viewed in the online issue, which is available at wileyonlinelibrary.com.]

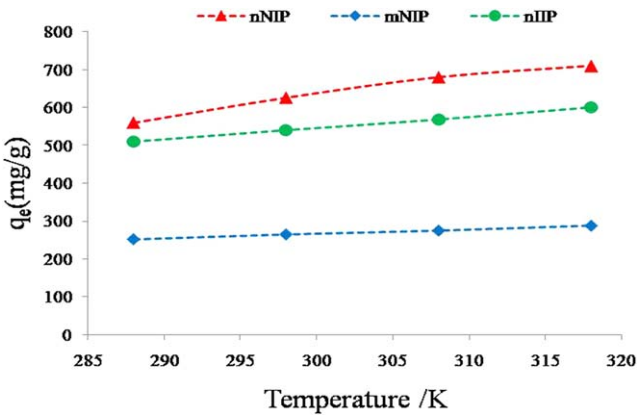

Figure 7. The effect of temperature on adsorption capacity. [Color figure can be viewed in the online issue, which is available at wileyonlinelibrary.com.]

Table IV. Thermodynamic Parameters of Fibrous Adsorbents for Pb(II) Adsorption (pH 5.8; Initial Pb(II) Concentration of 500 mg/L)

	ΔG (kJ/mol)			
Fibrous adsorbents	288 K	298 K	308 K	318 K
nNIP	−22.0	−22.7	−23.4	−24.3
nIIP	−18.9	−19.5	−20.2	−20.8
mNIP	−17.7	−18.2	−18.8	−19.5

nNIP, nIIP, and mNIP represent non-ion imprinted chelating nanofibers, Pb(II) ion-imprinted chelating nanofibers, and non-ion imprinted chelating microfibers, respectively.

diffusion of Pb(II) becomes much easier to surface of adsorbents. Secondly, the fiber membrane diffusion becomes easier because of the fibrous adsorbent swelling.

Thermodynamic parameters such as free energy changes (ΔG, kJ mol^{-1}) associated with sorption process were calculated from the following equations,[41] and the results are shown in Table III.

$$\Delta G = -RT\ln K \quad (13)$$

where the K (mL/g) is the adsorption equilibrium constant, which equals to Langmuir constant (K_L) related to the measure of affinity of the adsorbate for adsorbent[44] owing to adsorption process fitted particularly well with Langmuir model. ΔG is the Gibbs free energy change (kJ/mol). T denotes the absolute temperature, R is the universal gas constant.

According to data in Table IV, all the values of ΔG of tested adsorbents for Pb(II) sorption were negative, and the change in free energy increase with an increase of temperature, which suggested that the adsorption process is spontaneous and favorable at high temperature. This could be possibly because of activation of more sites on the surface of fiber membrane with rise in temperature.

Selective Adsorption

Selective adsorption of Pb(II)-IIP were carried out in the presence of competitive metal ions with same charge or similar ionic radius, for instance, the binary solutions of Pb(II)/Cu(II), Pb(II)/Ni(II), and Pb(II)/Cd(II). As shown in Table V, selectivity coefficients (k) of nNIP and mNIP for absorbing Pb(II) from binary ion solutions were much less than that of nIIP, which indicated that nIIP did generate high affinity binding sites for Pb(II) that were characteristically different from the randomly distributed functional groups in nNIP. The selectivity coefficient of nIIP for Pb(II) with respect to Cd(II) could reach 162.8, which was the highest selectivity coefficient to our knowlwdge.

Table V. Selective Adsorption of Pb(II) in the Presence of Competitive Ions (298 K)

	Fibers					
	mNIP		nNIP		nIIP	
Ions	k_d (L/mg)	k'	k_d (L/mg)	k'	k_d (L/mg)	k'
Pb(II)	3.901	2.818	0.809	0.757	6.544	47.442
Cu(II)	1.384		1.06		0.138	
Pb(II)	10.629	8.341	2.975	9.42	4.579	101.5
Ni(II)	1.274		0.316		0.045	
Pb(II)	9.326	3.721	1.83	6.257	4.897	162.81
Cd(II)	2.506		0.293		0.03	

nNIP, nIIP, and mNIP represent non-ion imprinted chelating nanofibers, Pb(II) ion-imprinted chelating nanofibers, and non-ion imprinted chelating microfibers, respectively.

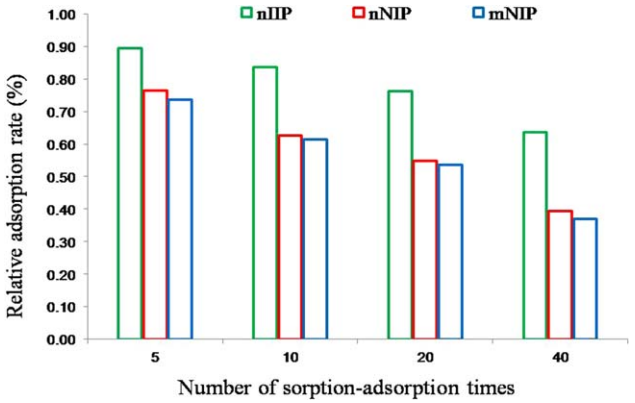

Figure 8. The relationship between the changes of adsorption capacity and adsorption/desorption cycles. [Color figure can be viewed in the online issue, which is available at wileyonlinelibrary.com.]

The difference of selectivity coefficients between nNIP and mNIP was not much significant as showed in Table V, because the major functional groups of raw materials of nNIP and mNIP were the same although the raw materials of mNIP containing some ester functional groups.

The findings from competitive adsorptions revealed that there are two important factors that determine selectivity. Firstly, the type of functional groups on adsorbent effects adsorption selectivity,[31] which might be explained with the theory of hard and soft acids and bases (HSAB)[45] as well as the crystal field theory.[46] Secondly, ion-imprinting technique plays a key role in adsorption selectivity, which is based on molecular imprinting technique resulting in significantly increasing selectivity owing to template-selective recognition sites and geometries.[15,20]

Regeneration Characteristics

Besides the aforementioned selectivity, reusability is also an important index, since it plays a key role in realizing the cost-efficiency of nIIP. The adsorption capacity and relative adsorption capacity of fibrous adsorbents versus adsorption/desorption cycles are presented in Figure 8. Generally, adsorption capacity of all tested adsorbents decreased with the increase of adsorption/desorption cycles. However, the relative adsorption capacity of nIIP was about 64% after 40 adsorption/desorption cycles, which was the highest among all the tested adsorbents, suggested that the reusability of nIIP was much better than that of lead ion-imprinted nanofibers reported by Li.[47] As a matter of fact, the difference between nIIP and lead ion-imprinted nanofibers reported by Li was the type and number of functional groups as well as imprinting technique,

the adsorption/desorption rate of nIIP is much higher that those of adsorbents prepared by classical ion imprinting technique.

In contrast to nIIP, adsorption capacity of nNIP and mNIP significantly decreased with the number of adsorption/desorption cycles increased, which might be ascribed to oxidation of amidoxime groups of adsorbents during adsorption/desorption process.[48] The regeneration data implied that nIIP possesses more chemical stability resulting from ion-imprinting and can be regenerated efficiently, and it is economically and technically potential to be applied for heavy metal polluted wastewater treatment and recovering pure metals.

CONCLUSIONS

In the present work, a novel surface nIIP has been successfully prepared via electrospinning and surface ion imprinting technique. The adsorption capacity and adsorption rate of nIIP were much higher and faster than that of mNIP. The adsorption of Pb(II) onto nIIP was well fitted with pseudo-second order kinetic and Langmuir model. The values of Gibbs free energy change derived from experimental data revealed that the adsorption process is spontaneous and favorable at high temperature. In addition, nIIP had the highest selectivity of tested fibrous adsorbents for Pb(II) in binary metal solution, the selectivity coefficients of Pb(II)/Cu(II), Pb(II)/Ni(II), and Pb(II)/Cd(II) were 47, 101, and 162, respectively. Besides, the stability and regeneration of nIIP were the best one among tested fibrous adsorbents after forty re-sorption cycles. The most prominent feature of nIIP prepared by electrospinning and surface ion imprinting technique are high selectivity in multi ions and stability in waste water. So there is a great application protential in recycling heavy or noble metals, separating and accumulating trace ions, and dealing with heavy metal polluted wastewater in a cost-efficent way.

ACKNOWLEDGMENTS

This research was supported by Guangdong Province of Ministry of Education, Ministry of Science and Technology Grants 2012A090300007 and 2012B090900015.

AUTHOR CONTRIBUTIONS

Lanyan Tong designed and performed all the experiments and wrote the manuscript; Professor Jida Chen supervised and revised the manuscript; Youyou Yuan, Zehua Cui, and Mianfu Ran synthesized Pb(II) ion-imprinted chelating nanofibers and characterization of samples; Qian Zhang and Juan Bu characterized the morphology of fibers and analyzed the experiments data; Professor Fengqing Yang reviewed and revised the manuscript; Xinhong Su and Huan Xu performed the adsorption experiments.

REFERENCES

1. Bai, L.; Hu, H. P.; Fu, W.; Wan, J.; Cheng, X. L.; Zhuge, L.; Xiong, L.; Chen, Q. Y. *J. Hazard. Mater.* **2011**, *195*, 261.
2. Caussy, D. *Ecotoxicol. Environ. Saf.* **2003**, *56*, 164.
3. Jain, C. K.; Ali, I. *Water Res.* **2000**, *34*, 4304.
4. Charlet, L.; Chapron, Y.; Faller, P.; Kirsch, R.; Stone, A. T.; Baveye, P. C. *Coord. Chem. Rev.* **2012**, *265*, 2147.
5. Kozlowski, H.; Luczkowski, M.; Remelli, M.; Valensin, D. *Coord. Chem. Rev.* **2012**, *256*, 2129.
6. Toscano, C. D.; Guilarte, T. R. *Brain. Res. Rev.* **2005**, *49*, 529.
7. Clarkson, T. W.; Magos, L. *Crit. Rev. Toxicol.* **2006**, *36*, 609.
8. Singh, A.; Kumar, D.; Gaur, J. P. *Water. Res.* **2012**, *46*, 779.
9. Liu, C. K.; Bai, R. B.; Ly, Q. S. *Water. Res.* **2008**, *42*, 1511.
10. Murthy, Z. V. P.; Chaudhari, L. B. *Chem. Eng. J.* **2009**, *150*, 181.
11. Ekmekyapar, F.; Aslan, A.; Bayhan, Y. K.; Cakici, A. *J. Hazard. Mater.* **2006**, *137*, 293.
12. Laus, R.; Costa, T. G.; Szpoganicz, B.; Favere, V. T. *J. Hazard. Mater.* **2010**, *183*, 233.
13. Ren, Y. M.; Wei, X. Z.; Zhang, M. L.; Zhang, M. L. *J. Hazard. Mater.* **2008**, *158*, 14.
14. Luo, X. B.; Luo, S. L.; Zhan, Y. C. *J. Hazard. Mater.* **2011**, *192*, 949.
15. Li, T. Y.; Chen, S. X.; Li, H. C.; Li, Q. H.; Wu, L. *Langmuir* **2011**, *27*, 6753.
16. Zhang, M. L.; Zhang, Z. H.; Liu, Y. N.; Yang, X.; Chen, J. T.; Yao, S. Z. *Chem. Eng. J.* **2011**, *178*, 443.
17. Li, Z. C.; Fan, H. T.; Zhang, Y.; Chen, M. X.; Yu, Z. Y.; Cao, X. Q.; Sun, T. *Chem. Eng. J.* **2011**, *171*, 703.
18. Li, Y.; Yue, Q. Y.; Gao, B. Y. *J. Hazard. Mater.* **2010**, *178*, 455.
19. Gao, B. J.; An, F. Q.; Zhu, Y. *Polymer* **2007**, *48*, 2288.
20. Wang, L. M.; Zhou, M. H.; Jing, Z. H.; Zhong, A. F. *Microchim. Atca.* **2009**, *165*, 367.
21. Zhu, L. Y.; Zhu, Z. L.; Zhang, R. H.; Qiu, Y. L. *J. Environ. Sci.* **2011**, *23*, 1955.
22. Liu, B. J.; Lv, X.; Meng, X. H.; Yu, G. L.; Wang, D. F. *Chem. Eng. J.* **2013**, *220*, 412.
23. Liu, Y.; Liu, Z. C.; Gao, J.; Dai, J. D.; Han, J.; Wang, Y.; Xie, J. M.; Yan, Y. S. *J. Hazard. Mater.* **2011**, *186*, 197.
24. Khajeh, M.; Heidari, Z. S.; Sanchooli, E. *Chem. Eng. J.* **2011**, *166*, 1158.
25. Nasouri, K.; Bahrambeygi, H.; Rabbi, A.; Shoushtari, A. M.; Kaflou, A. *J. Appl. Polym. Sci.* **2012**, *126*, 127.
26. Yu, H.; Guo, J.; Zhu, S. Q. *Mater. Lett.* **2012**, *74*, 247.
27. Huang, L. W.; Manickam, S. S.; McCutcheon, J. R. *J. Membr. Sci.* **2013**, *436*, 213.
28. Saeed, K.; Haider, S.; Oh, T. J.; Park, S. Y. *J. Membr. Sci.* **2008**, *322*, 400.
29. Neghlani, P. K.; Rafizadeh, M.; Taromi, F. A. *J. Hazard. Mater.* **2011**, *186*, 182.
30. El-Khouly, A. S.; Takahashi, Y.; Saafan, A. A. *J. Appl. Polym. Sci.* **2011**, *120*, 866.
31. Coskun, R.; Soykan, C. *J. Appl. Polym. Sci.* **2009**, *112*, 1798.
32. Zhang, X.; Jin, X. Y.; Xu, C. Y.; Shen, X. Y. *J. Appl. Polym. Sci.* **2013**, *128*, 3665.

33. Monier, M.; Ayad, D. M.; Wei, Y.; Sarhan, A. A. *J. Hazard. Mater.* **2010**, *177*, 962.
34. Dai, S.; Burleigh, M. C.; Shin, Y. S.; Morrow, C. C.; Barnes, C. E.; Xue, Z. *Angew. Chem. Int. Edit.* **1999**, *38*, 1235.
35. Kampalanonwat, P.; Supaphol, P. *ACS Appl. Mater. Interfaces* **2010**, *2*, 3619.
36. Ng, J. C. Y.; Cheung, W. H.; McKay, G. *J. Colloid Interface Sci.* **2002**, *255*, 64.
37. Demirbas, E.; Dizge, N.; Sulak, M. T.; Kobya, M. *Chem. Eng. J.* **2009**, *148*, 480.
38. Hall, K. R.; Eagleton, L. C.; Acrivos, A.; Vermeulen, T. *Ind. Eng. Chem. Fundam.* **1966**, *5*, 212.
39. Wang, X.; Wang, L. Y.; He, X. W.; Zhang, Y. K.; Chen, L. X. *Talanta* **2009**, *78*, 327.
40. Azizian, S. *J. Colloid Interface Sci.* **2004**, *276*, 47.
41. Chen, J. H.; Xing, H. T.; Guo, H. X.; Li, G. L.; Weng, W.; Hu, S. R. *J. Hazard. Mater.* **2013**, *248*, 285.
42. Iftikhar, A. R.; Bhatti, H. N.; Hanifa, M. A.; Nadeem, R. *J. Hazard. Mater.* **2009**, *161*, 941.
43. Özacara, M.; Sengilb, I. A.; Türkmenler, H. J. *Chem. Eng. J.* **2008**, *143*, 32.
44. Buhani; Narsito; Nuryono. *Desalination* **2010**, *251*, 83.
45. Pearson, R. G. *J. Am. Chem. Soc.* **1963**, *85*, 3533.
46. Leavitt, R. P. *J. Chem. Phys.* **1982**, *77*, 1661.
47. Li, Y.; Qiu,T. B.; Xu, X. Y. *Eur. Polym. J.* **2013**, *49*, 1487.
48. Lin, W. P.; Lu, Y.; Zeng, H. M. *J. Appl. Polym. Sci.* **1993**, *49*, 1635.